BMC Ecology and Evolution

RESEARCH

Open Access

Inferring the energy cost of resistance to parasitic infection and its link to a trade-off

Frédéric Douhard[1*], Carole Moreno-Romieux[1^] and Andrea B. Doeschl-Wilson[2]

Abstract

Background In infected hosts, immune responses trigger a systemic energy reallocation away from energy storage and growth, to fuel a costly defense program. The exact energy costs of immune defense are however unknown in general. Life history theory predicts that such costs underpin trade-offs between host disease resistance and other fitness related traits, yet this has been seldom assessed. Here we investigate immune energy cost induced by infection, and their potential link to a trade-off between host resistance and fat storage that we previously exposed in sheep divergently selected for resistance to a pathogenic helminth.

Results To this purpose, we developed a mathematical model of host-parasite interaction featuring individual changes in energy allocation over the course of infection. The model was fitted to data from an experimental infectious challenge in sheep from genetically resistant and susceptible lines to infer the magnitude of immune energy costs. A relatively small and transient immune energy cost in early infection best explained within-individual changes in growth, energy storage and parasite burden. Among individuals, predicted responses assuming this positive energy cost conformed to the observed trade-off between resistance and storage, whereas a cost-free scenario incorrectly predicted no trade-off.

Conclusions Our mechanistic model fitting to experimental data provides novel insights into the link between energy costs and reallocation due to induced resistance within-individual, and trade-offs among individuals of selected lines. These will be useful to better understand the exact role of energy allocation in the evolution of host defenses, and for predicting the emergence of trade-offs in genetic selection.

Keywords Resource allocation trade-offs, Host resistance, Mathematical modelling

Background

The costs of immunity remain a central and long-standing question in evolutionary ecology, medical and animal sciences [1–3]. In particular, a fundamental life history assumption is that the evolution of host defense strategies against pathogens critically depends on energy and other nutrient costs to deploy an immune response [4, 5]. Immune costs induced upon infection have also been associated with a diversion of nutritional energy away from storage, reproductive and growth processes in order to meet the concurrent energy demands of the infected host [6–8]. According to the allocation hypothesis, such energy reallocation could instigate trade-offs between host resistance (i.e. the ability to limit within-host pathogen replication) and other fitness-related traits such as growth or reproduction [9, 10]. In particular, those trade-offs are expected to arise when energy supply falls short, such as during infection-induced anorexia [11, 12]. However, in many cases trade-offs are not detected

Carole Moreno-Romieux is deceased.

*Correspondence:
Frédéric Douhard
frederic.douhard@inrae.fr
[1] GenPhySE, Université de Toulouse, INRAE, ENVT, Castanet-Tolosan F-31326, France
[2] The Roslin Institute and Royal (Dick) School of Veterinary Studies, University of Edinburgh, Edinburgh, UK

[13–18], putting the concept of costly immune defense into question [19].

Trade-offs can be undetected when hosts manage to mitigate the negative fitness consequences of an energy costly immune response. For instance, hosts can simultaneously adjust their energy intake or other components of their energy budget to meet the extra energy demand of immune activation [20]. Yet, quantifying the immune energy demand remains challenging. Most previous attempts have relied on changes in the rate of energy use for basal metabolism (e.g. resting metabolic rate) in infected hosts [7, 21, 22]. However, even though infection should lead to an increase in metabolic rate, the direction and the magnitude of this effect seem actually highly inconsistent across studies and host-parasite systems [23]. In some cases, hosts even enter into an hypometabolic state along with infection-induced anorexia to promote particular resistance [24] or tolerance mechanisms [12]. In certain of those situations, negative effects on fitness-related traits seem to be primarily caused by this reduction in intake rather by the energy costs of immune deployment [25, 26]. Furthermore, since metabolic trajectories after pathogen exposure strongly depend on host-parasite dynamics [27], it is increasingly clear that attempts to measure the costs of immune activation should consider the changes in energy intake and energy expenditure triggered by the immune response over the course of infection.

In this study, we investigated host resistance dynamics, assuming that the level of resistance reflects the strength of an immune response deployed by the host. Under this assumption, we investigated energy-allocation trade-offs involving host resistance by answering two questions: (Q1) Does host resistance entail a substantial induced energy cost over the course of a parasitic infection in a vertebrate host? (Q2) If so, does this energy cost conform to an observed trade-off between host resistance and fat storage?

To this purpose, we used experimental data of domestic sheep artificially challenged with the blood-feeding gastrointestinal nematode *Haemonchus contortus*. In this model system, complex immune effector mechanisms [28–30] confer genetic differences in host resistance to infection [13, 15]. In our studies, hosts were from lines divergently selected for resistance to short-term infectious challenge with *H. contortus*, so that responses of resistant (R) and susceptible (S) hosts should reflect a genetic difference in the strength of induced immunity against this specific parasite [31]. We previously detected a trade-off among lines between host resistance (using parasite fecal egg counts (FEC) as proxy) and the gain in fat reserves (using backfat thickness (*BFT*) as proxy), with the R line having significantly lower *FEC* and lower *BFT* than the S line [32]. However, a statistical analysis of the traits dynamics observed during the infection (Fig. 1Ai-v) could not determine if the reduced fat accumulation of R sheep compared with S sheep can be fully explained by their lower feed intake (i.e. without the need to divert energy from fat storage towards immunity to satisfy immune energy costs), or if it partly resulted from an energy allocation away from fat deposition to parasite-specific, potentially costly, immunity. It is not a priori obvious which of the two scenarios would best conform to the observed trade-off (Fig. 1B). In this study we developed a mechanistic mathematical model of host-parasite interactions featuring dynamic changes in energy allocation. We fitted this model to the experimental data to answer the biological questions above. Thereby, we tested two alternative hypotheses (Fig. 1B): (H1) there are non-negligible immune energy costs associated with host resistance, and the observed lower fat storage in the R line is the consequence of energy allocated away from fat storage to immunity to meet the higher immune energy demands in the R line, vs. (H0) immune energy costs are negligible, and the observed lower fat storage in the R line is the direct consequence of the more strongly reduced feed intake as a by-product of infection.

Methods

Inference approach and hypotheses

To test hypotheses H0 and H1, we combined previous experimental data with dynamic mathematical modelling. In brief, we developed two dynamic mechanistic models: one of host energy budget (using energy intake as a known model input) and one of host-parasite interaction, that were interconnected through a varying, potentially null, energy flow from feed to immunity ($E_{immunity}$) (see details in *Model description*). The coupled model (Fig. 2) was fitted to longitudinal data for each individual sheep (n = 42) allowing for individual variation in two virtual immune responses associated to specific stages of nematode infection [28, 30]: one acting early against larvae establishment (I_E) and one acting later against parasite fecundity (I_F). The unknown unitary energy cost associated with these responses (e_{I_E} and e_{I_F}, respectively) were used to test H0 and H1. They were assumed constant among individuals, just like the energy costs for maintenance, lipid and protein biosynthesis known from the literature [33]. Energy allocated to immunity was thus defined as $E_{immunity} = e_{I_E} \cdot I_E + e_{I_F} \cdot I_F$.

By fitting the mechanistic model to the data, immune energy costs and the value of other parameters controlling the strength of I_E and I_F were inferred. In support of H_1, we predicted that:

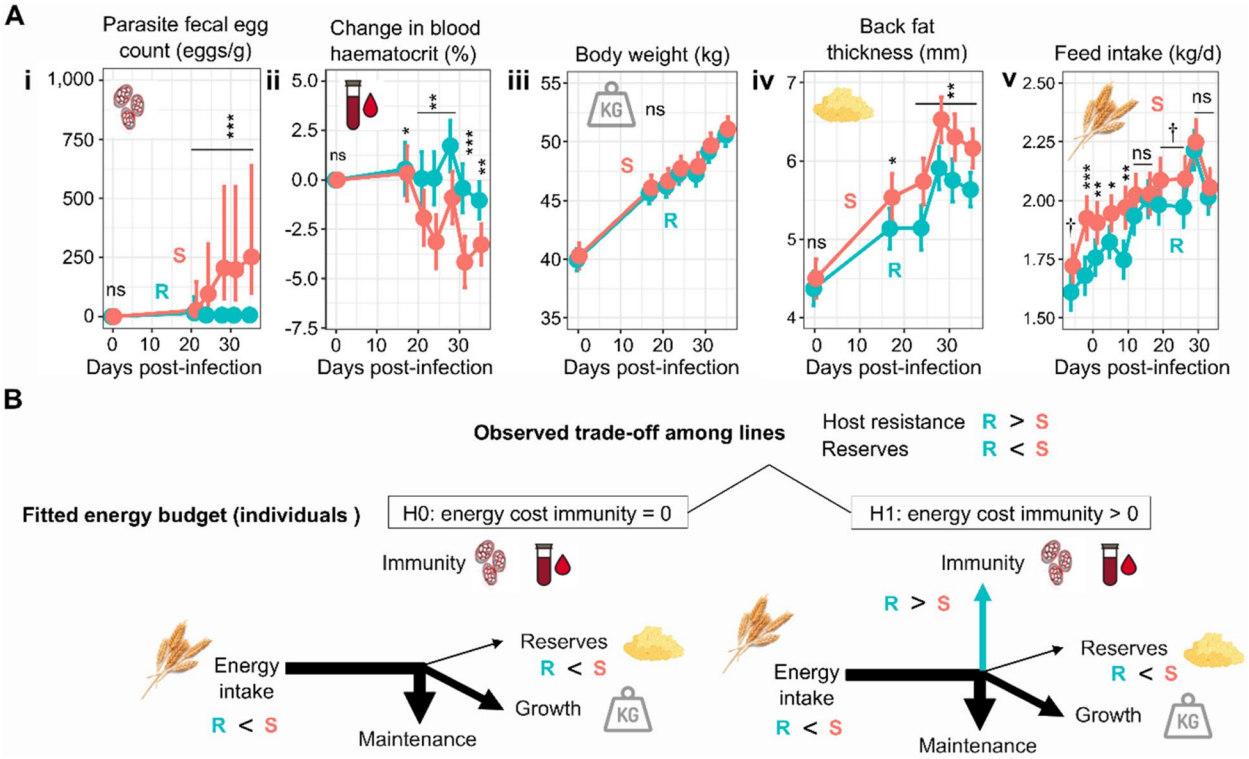

Fig. 1 Experimental data integrated in this study to infer the energy cost of immunity. **A** Data represent responses to a parasitic challenge (10,000 third-stage larvae of *Haemonchus contortus* per animal given orally) observed in growing female sheep resistant (R; $n = 21$) or susceptible (S; $n = 21$) to infection with *H. contortus*. It supports a trade-off between host resistance (i, ii) and the gain in fat reserves (iv), possibly mediated by feed intake in early infection (v). In addition, an energy cost of parasite-specific immunity may contribute to the trade-off between lines (hypothesis H1), or not (hypothesis H0). **B** To test hypotheses H0 and H1, a dynamic mechanistic model of energy budget coupled with host–pathogen interaction was fitted individually to the observed data. Fig Ai-v were modified from [32]. Points represent adjusted means with their error bars representing 95% confidence interval and asterisks indicate statistical difference between lines (ns: $p > 0.1$; †: $p < 0.1$; *: $p < 0.05$; **: $p < 0.01$; ***: $p < 0.001$)

(i) positive values of population energy cost parameters e_{I_E} and e_{I_F} best explain the observed data,
(ii) the R and S lines differ in terms of energy allocation strategies between host resistance ($E_{immunity}$) and host growth during infection,
(iii) individual parameters controlling the strength of I_E and I_F differ between the R and S lines,
(iv) energy allocation can generate a trade-off between host resistance and fat reserves, and
(v) individual growth parameters out-of-infection do not differ between lines.

Experimental data

We used data from an artificial infestation experiment in growing female lambs from two lines divergently selected for resistance to *H. contortus*. Both lines originated from a prolific meat sheep breed (Romane) bred indoor at INRAE experimental facilities. Sheep were selected on their resistance to parasites based on *FEC* measures, following a unique protocol comprising two successive infections as outlined in detail in [34]. In the initial population, 274 naïve lambs were infected with a single dose of 10,000 third stage larvae (L3) of *H. contortus* to stimulate a primary immune response; 4 weeks later they were treated (0.2 mg/kg of live weight of ivermectin; Oramec, Boerhinger Ingelheim, Lyon, France); after 2 weeks of recovery they were re-infected with a single dose of 10,000 L3 to simulate a secondary immune response and finally treated 5 weeks later. At the end of first and second infection, *FEC* was recorded just before treatment and those measures were combined to estimate animal breeding values for resistance used as selection criterion to generate the two divergently selected lines.

This study then used data from 42 ewe lambs from the second generation (G_2) of divergent selection for resistance (R = low *FEC*, $n = 21$) or susceptibility (S = high *FEC*, $n = 21$). At G_2, the divergence in *FEC* between R and S sheep reached a 1.9 phenotypic SD (σ_p) and 3.8 genetic SD (σ_g) from the mean *FEC* of initial population (G_0). Specifically, female G_2 lambs were infected early to stimulate a primary immune response, and again at 4

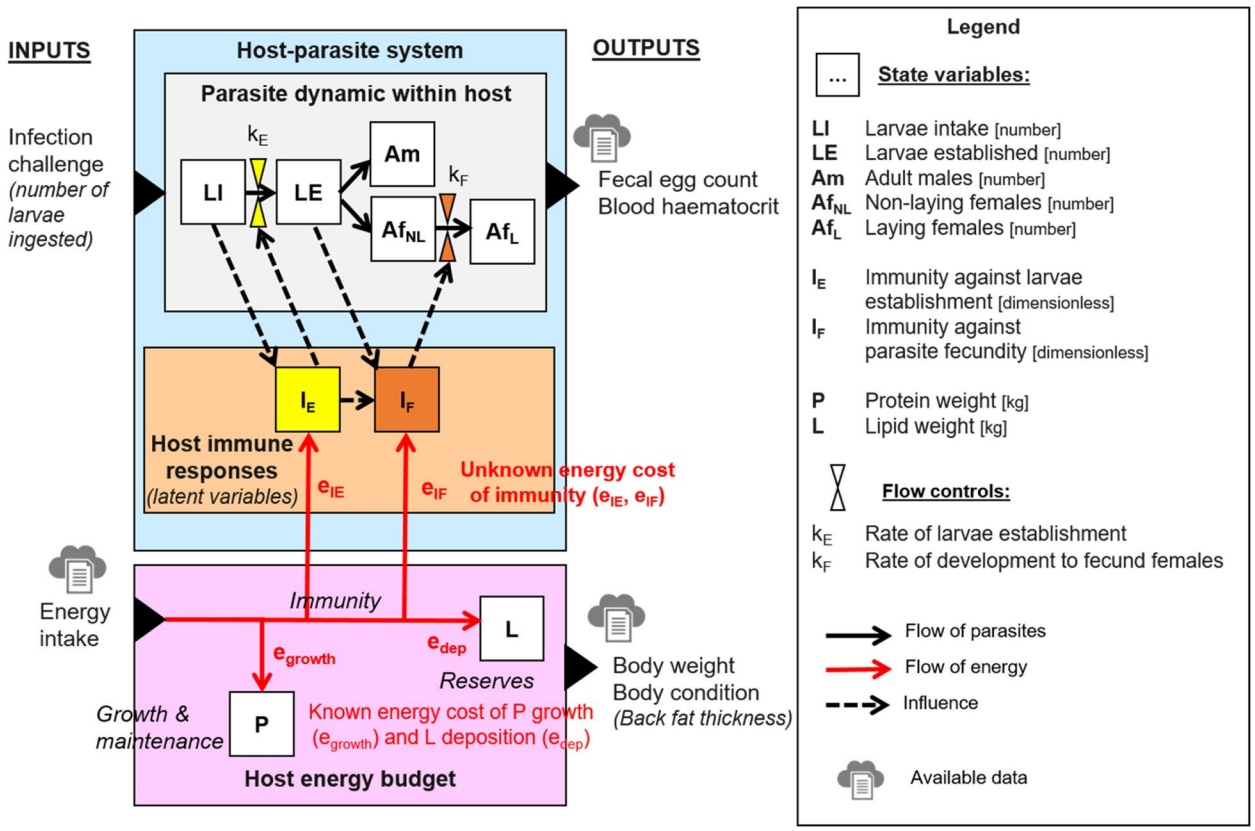

Fig. 2 Conceptual diagram of the host-parasite model coupled with a model of host energy budget to estimate the energy cost of immune responses from experimental data

months of age, following the same infection protocol as described above, except that the first dose was of 3,500 L3/sheep to limit the potential negative consequences of infection on fertility at first mating (at 8–9 months of age). During the infection, lambs were fed ad libitum with a protein-rich concentrate (176.6 g of crude protein/kg of dry matter) and straw so that protein was not nutritionally limiting compared with energy. The longitudinal data collected during the second infection were then used in this study to calibrate the host-parasite interaction model. Data included voluntary concentrate intake (in kg/d; measured daily with automatic feeders) and five other traits measured at day 0, 17, 24, 28, 31, and 35 post-infection: *FEC* (in egg/g; measured by the modified McMaster technique), blood haematocrit (in %; measured by microhaematocrit centrifugation technique), body weight (in kg), back fat thickness (*BFT*, in mm; measured by ultrasound scan on both sides at the 12th– 13th lumbar vertebra (Easi- Scan™, IMV imaging)). Those traits could be linked to the model as shown in Fig. 1. E_{intake} was estimated from concentrate intake and diet characteristics (Table 1) assuming that concentrate was the main source of feed energy (i.e. straw intake was considered as negligible).

Model description

Overview

In accordance with experimental data, the model represents a growing non-reproducing sheep fed ad libitum with a protein-rich diet, infected with a single dose of L3 (Fig. 2). Both the infection challenge dose and energy intake are assumed to be known and can be used as a model input. The host-parasite system includes two components: the parasite development within the host (from third stage infective larvae *LI* to reproducing adults *Am* andAf_{NL}), and the host immune responses against the infection. As for prey-predator models [41], these two components interact dynamically as parasitic load triggers the immune responses which in turn, act on parasite development. The immunological mechanisms by which animals have or acquire resistance to haemonchosis are highly complex and still largely unraveled [28]. Here the two latent immune response variables, I_E and I_F reflect an action on two key stages of parasite

Table 1 List of model parameters

Parameter	Definition	Value	Source
Parasites development			
μ_{LI}; μ_{LE}; μ_{Am}; $\mu_{Af_{NL}}$; μ_{Af_L}	Mortality rates [per day] of *LI*, *LE*, and of *Am*, Af_{NL}, Af_L	0.18; 0.01; 0.015	[35]
p_{Am}	Proportion of LE that are males (the remaining proportion 1—$p_{Am}$are females)	0.5	assumed
k_{E_0}; k_{F_0}	Maximum transition rates from *LI* to *LE* (establishment), and from Af_{NL} to Af_L (fecundity)	2; 0.3	assumed
k_A	Constant transition rate from *LE* to *Am* and Af_{NL}	0.62	assumed
τ_{LI};τ_{LE}	Minimum time delay (in days) from ingestion to establishment site, and from establishment to emergence	2; 15	[35]
F_0	Maximum fecundity rate per capita (number of eggs per day and per adult female)	7000	[36]
ω_{LE}; ω_{Am}; $\omega_{Af_{NL}}$; ω_{Af_L}	Loss in HE per capita for parasite categories *LE*, *Am*, Af_{NL}, and Af_L, respectively	($\times 1^{e-5}$) 15; 50; 50; 110	[37]
Host immune response			
$l_{E0.5}$; $l_{F0.5}$	Levels of l_E and l_F at which k_E and k_F respectively, are reduced of 50%	5	assumed
αk_E; αk_F	Shape factors of immune effects on k_E and k_F	3	assumed
φ_{l_E}; φ_{l_F}	Per capita replication rates of l_E and l_F, respectively	*assumed to vary between individuals; estimated (individual level)*	
αl_E	Shape factor of parasite effect (*LI*) on l_E replication	3	assumed
$LI_{0.5}$	Level of *LI* at which l_E replication is at 50% of its maximum	3000	assumed
l_{E_0}; l_{F_0}	Baseline levels of l_E and l_F	1	assumed
β_{l_E}; β_{l_F}	Per capita loss rates of l_E and l_F, respectively	0.05	assumed
Host energy budget			
α_{P_m}	Scaling exponent ofP_m	0.27	[33, 38]
P_m	Protein weight at maturity [kg]	*assumed to vary between individuals; estimated (individual level)*	
L_m	Lipid weight at maturity [kg]		
β_P	Relative protein growth rate from birth to maturity [$kg^{\alpha_{P_m}}.day^{-1}$]		
β_P^*	Relative protein growth rate during infection [$kg^{\alpha_{P_m}}.day^{-1}$]		
β_{Wool}	Relative wool growth rate [day^{-1}]		
e_{growth}; e_{maint}; e_{dep}; e_{mob}	Unitary energy costs (in MJ/kg) of protein growth, protein maintenance, lipid deposition, and lipid mobilization, respectively	56; 1.63; 50; 39.6	[33, 38]
e_{l_E}; e_{l_F}	Unitary energy costs (in MJ/unit) of immune responses l_E and l_F, respectively	*estimated (population level)*	
Observed host traits			
HE_0	Baseline level of*HE*[%]	*assumed to vary between individuals; estimated (individual level)*	
β_{HE}	Per loss rate of *HE* not due to infection	0.16	assumed
γ_{Ash}; γ_{Water}	Fixed ratio *Ash:P* and *Water:*P_m, respectively	0.211; 3.25	[33, 38]
α_{Water}	Scaling factor of protein maturity determining the proportion of body water	0.815	[33, 38]
a_{Gut_Fill}; b_{Gut_Fill}	Coefficients to predict *Gut_Fill* from *Feed_Energy*	11; 0.467	[39]
a_{BFT}; b_{BFT}; c_{BFT}	Coefficients to predict *BFT*	−4.01; 0.56; 1.52	[40]
DMC_{Feces}	Dry matter content of the feces	0.35	assumed
Diet characteristics			
DMC_{Feed}	Dry matter content of the feed	0.88	*known inputs*
DMD_{Feed}	Dry matter digestibility of the feed	0.76	
MEC_{Feed}	Metabolizable energy content of the feed (MJ/kg of DM)	7.7	

development: I_E limits the establishment of infective L3 larvae (k_E), and, I_F limits the reproductive maturation of adult females (k_F)).

For modelling energy budget, we assumed that protein accretion (P) to reach mature size drives body growth and remains unaffected by the early stages of infection. Indeed, dietary protein supplementation is known to favor the development of immunity [42, 43] but this type of effect only seems to occur once the nutritional requirements for growth are fulfilled [44]. Excess energy (not used for protein growth or maintenance) then fuels body lipid deposition (L) and leads to change in body reserves. Further, just as the synthesis and maintenance of a gram of protein or of lipid has an energy cost (e.g. e_{growth} or e_{dep} in Table 1), we considered that energy costs may also exist for both types of immune responses (e_{I_E} or e_{I_F} in Table 1). However, in contrast to e_{growth} or e_{dep} whose values are relatively well-known from the literature (Table 1), the values of e_{I_E} or e_{I_F} are unknown (Fig. 2).

In order to assess if immune responses contribute significantly to the energy budget and to estimate the corresponding energy costs (e_{I_E} and e_{I_F}), the model was fitted to experimental data and the goodness of fit was assessed both at the individual and at the population level. At the individual level, blood haematocrit and fecal egg count measures were used to indirectly estimate the magnitudes of the host immune responses I_E and I_F. Simultaneously, data on feed intake, body growth and reserves were used to estimate the components of the energy budget of each infected sheep, specifically their protein growth rate. Whilst the magnitude of the host immune response and energy budget vary both over time within an individual, and among individuals, the energy costs associated with the synthesis and maintenance of a gram of protein or of lipid e_{growth} or e_{dep}, and of e_{I_E} or e_{I_F} associated with one unit measure of I_E and I_F, respectively, were assumed to be constant among individuals. Hence, we repeated individual parameter estimations using different fixed values of e_{I_E} and e_{I_F} and looked for the best average goodness of fit at the population level (Fig. 3). In particular, if the best fit was obtained without immune energy cost (i.e. using $e_{I_E} = 0$ and $e_{I_F} = 0$), this would support the hypothesis that body growth and host resistance are nutritionally independent. In contrast, positive estimates of e_{I_E} or e_{I_F} would support the hypothesis that an energy allocation trade-off can occur between host resistance and body reserves.

Parasites dynamics within-host

The model describes the successive stages of parasite development within the host, from third stage larvae intake (LI) to fourth-stage larvae established in the abomasum (LE), and then from LE to adult fifth stage males (Am) or females (Af). Within females, the transition between non-laying (Af_{NL}) to laying females (Af_L) is represented as this last transition towards the most pathogenic stage largely determines the severity of the infection.

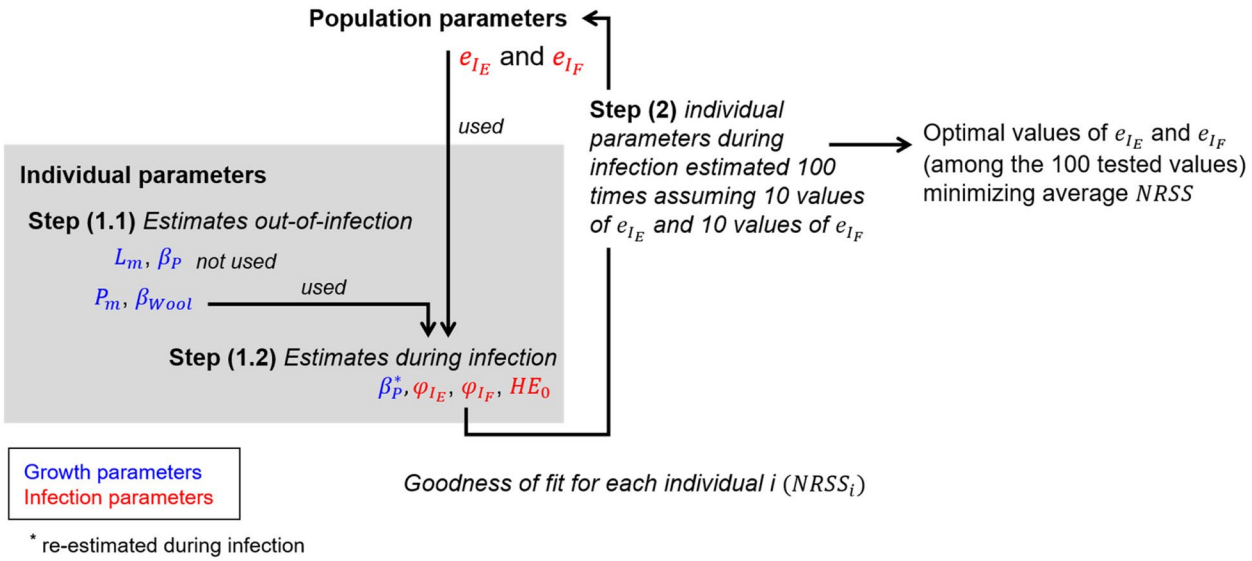

Fig. 3 Workflow of the model parameter estimation. Grey box indicates the two steps of individual parameter estimation (1.1 and 1.2). Step (2) iterates the process 100 times to determine the optimal values of energy costs of immunity against *Haemonchus contortus* infection. See Table 1 for parameter definition

The infection dynamics from the day of inoculation ($t=0$ and LI equal to initial dose LI_0) onwards is described by the following system of ordinary differential equations:

$$\frac{dLI}{dt} = -(\mu_{LI} + k_E) \cdot LI \quad (1)$$

where $k_E = 0$ if $t \leq \tau_{LI}$

$$\frac{dLE}{dt} = k_E \cdot LI - (\mu_{LE} + k_A) \cdot LE \quad (2)$$

where $k_A = 0$ if $t \leq \tau_{LE}$

$$\frac{dAm}{dt} = p_{Am} \cdot k_A \cdot LE - \mu_{Am} \cdot Am \quad (3)$$

$$\frac{dAf_{NL}}{dt} = (1 - p_{Am}) \cdot k_A \cdot LE - (\mu_{Af_{NL}} + k_F) \cdot Af_{NL} \quad (4)$$

$$\frac{dAf_L}{dt} = k_F \cdot Af_{NL} - \mu_{Af_L} \cdot Af_L \quad (5)$$

where k_E, k_A and k_F are transition rates that determine parasites establishment, development and fecundity and μ parameters are stage-specific mortality rates. Parasite sex is considered when parasites become adults, with p_{Am} indicating the proportion of males. Among the different stages of the parasitic phase, larvae establishment, adult fecundity, and adult mortality are considered to be key targets of the host immune system [44]. Here we considered immune effects on parasite establishment and fecundity (k_E and k_F) during the first stages of infection that we studied experimentally, and assumed constant mortality rates (μ) and rate of development from L4 to adults (k_A). Establishment rate k_E and female transition rate k_F were considered at maximum values k_{E_0} and k_{F_0} in the absence of any immune effect, and their values were reduced proportionally to the magnitude of specific immune responses I_E and I_F, respectively (further details in section '*Host immune responses*'). Moreover, there is a minimum time τ_{LI} required by ingested third-stage larvae (LI) before reaching host abomasum and establishment, and then a minimum time τ_{LE} to transform into adult fifth stage (Am or Af_{NL}). Thus, k_E and k_A were set to 0 when $t \leq \tau_{LI}$ and when $t \leq \tau_{LE}$, respectively.

Female worm fecundity is closely related to their body size which increases as they grow. To simplify we assumed that Af_{NL} represents an average worm of constant size and fecundity F_0 (i.e. average laying rate) so that the inverse of k_F corresponds to the average development time to reach that size and lay eggs. Thereby, immune influence on k_F controls whole population fecundity, that is the total egg excretion: $Af_L \cdot F_0$.

In order to fit the model to the experimental data, the dynamics of fecal egg counts (FEC) and blood haematrocit level (HE) was also modelled. Specifically, FEC (eggs number excreted per day and per gram of feces) was defined in relation to the weight of feces produced daily by the host ($Feces$) as follows:

$$FEC = \frac{AF_L \cdot F_0}{Feces} \quad (6)$$

where $Feces$ is determined by diet characteristics (cf. Table 1) and FI (in kg so multiplied by 1,000 to convert it into grams).

$$Feces = \frac{FI \cdot DMC_{Feed} \cdot (1 - DMD_{Feed})}{DMC_{Feces}} \cdot 1000 \quad (7)$$

Time change in HE was defined by a constant replication rate α_{HE} and a per capita loss β_{HE} under non-challenging conditions. For better ease of parameterization, we defined HE_0 as the equilibrium level of HE that equals β_{HE}/α_{HE} in the absence of infection. Under infectious challenge, HE dynamics is also affected by parasitic consumption. Blood haematocrit (HE) was negatively affected by the total number of parasites. This loss was assumed to depend on the parasitic loads associated with the different established parasitic stages (LE, Am, Af_{NL} and Af_L) and on the corresponding stage-specific effects ω:

$$\frac{dHE}{dt} = \beta_{HE} \cdot (HE_0 - HE) - (\omega_{LE} \cdot LE + \omega_{Am} \cdot Am + \omega_{Af_{NL}} \cdot Af_{NL} + \omega_{Af_L} \cdot Af_L) \quad (8)$$

Our model accounts for the fact that HE and FEC dynamics may reflect different biological processes that can be differently controlled by host immunity (e.g. HE can decrease due to some worm burden but this does not necessarily implies a correlated increase in FEC if for instance the host develops a strong anti-fecundity response). Nevertheless, HE and FEC may still be moderately to strongly negatively correlated in accordance with the literature [45].

Host immune responses

Effects of the host immune responses I_E and I_F on k_E and k_F, respectively, were assumed to follow a sigmoidal pattern [41, 46], so that at low levels of immunity the responses are relatively inefficient (e.g. in naïve animals) whereas they saturate at high levels, for instance due to time constraints on immune cells to neutralize parasites. In model terms, the maximum (k_{E_0} and k_{F_0}), the inflection point ($I_{E_{0.5}}$ and $I_{F_{0.5}}$) and the shape (αk_E and αk_F) were determining sigmoidal patterns as follows:

$$k_E(I_E) = \frac{1}{\left(\frac{I_E}{I_{E_{0.5}}}\right)^{\alpha k_E} + 1} \cdot k_{E_0} \quad (9)$$

and

$$k_F(I_F) = \frac{1}{\left(\frac{I_F}{I_{F_{0.5}}}\right)^{\alpha k_F} + 1} \cdot k_{F_0} \quad (10)$$

The development of immune response against parasite establishment I_E was assumed to be triggered by the intake of L3 larvae (LI). As for the immune effect on parasite we assumed that the increase in the replication rate of I_E according to LI followed a sigmoidal pattern:

$$\frac{dI_E}{dt} = \left(\varphi_{I_E} \cdot \frac{1}{\left(\frac{LI_{0.5}}{LI}\right)^{\alpha I_E} + 1} \cdot I_E\right) - \beta_{I_E} \cdot \left(I_E - I_{E_0}\right) \quad (11)$$

The early immune response I_E, in interaction with the number of L4 established larvae (LE) were then assumed to elicit the immune response I_F against the reproduction of adult parasites as follows:

$$\frac{dI_F}{dt} = \left(\varphi_{I_F} \cdot \left(I_E - I_{E_0}\right) \cdot LE\right) - \beta_{I_F} \cdot \left(I_F - I_{F_0}\right) \quad (12)$$

Of note, an increase in φ_{I_E} will lead to an increase in I_E (Fig. 4A), as well as in I_F in case of positive φ_{I_F} (Fig. 4C), respectively. Whereas φ_{I_F} only affects I_F (Fig. 4B) and has no effect on I_E, φ_{I_E} has a non-linear effect on I_F (Fig. 4C). For low values of φ_{I_E}, I_E increases faster than LE declines (i.e. the product $\left(I_E - I_{E_0}\right) \cdot LE$ increases) whereas for higher values of φ_{I_E}, I_E effectively reduces LE which then subsequently reduces the immune response I_F (as a stimulation of a strong I_F would be pointless). This non-linear effect is more pronounced for higher values of φ_{I_F} (Fig. 4C).

Host energy budget

The host energy balance (EB) was defined as the energy intake minus the sum of the different energy requirements:

$$EB = E_{intake} - (E_{growth} + E_{maint} + E_{immunity}) \quad (13)$$

and then determined the rate of lipid (L) deposition or mobilization:

$$\frac{dL}{dt} = \begin{cases} e_{dep} \cdot EB & \text{if EB} \geq 0 \\ e_{mob} \cdot EB & \text{otherwise} \end{cases} \quad (14)$$

This model was based on a previous nutritional growth model [33], except that we added the component $E_{immunity}$ and sought to estimate its parameters based on our experimental data. Specifically, $E_{immunity}$ was considered as a weighted sum of immune responses I_E and I_F:

$$E_{immunity} = e_{I_E} \cdot I_E + e_{I_F} \cdot I_F \quad (15)$$

where the weighing factors e_{I_E} and e_{I_F} represent the energy costs per unit of immune component I_E and I_F. Their values were assumed to be constant among individuals.

In the EB equation, E_{intake} was obtained using individual spline estimate of FI according to the time of infection and assuming constant feed characteristics:

$$E_{intake} = FI \cdot DMC_{Feed} \cdot MEC_{Feed} \quad (16)$$

The energy requirement for protein accretion (E_{growth}) was driven by the temporal changes in carcass protein (P) and $Wool$:

$$E_{growth} = e_{growth} \cdot \left(\frac{dP}{dt} + \frac{dWool}{dt}\right) \quad (17)$$

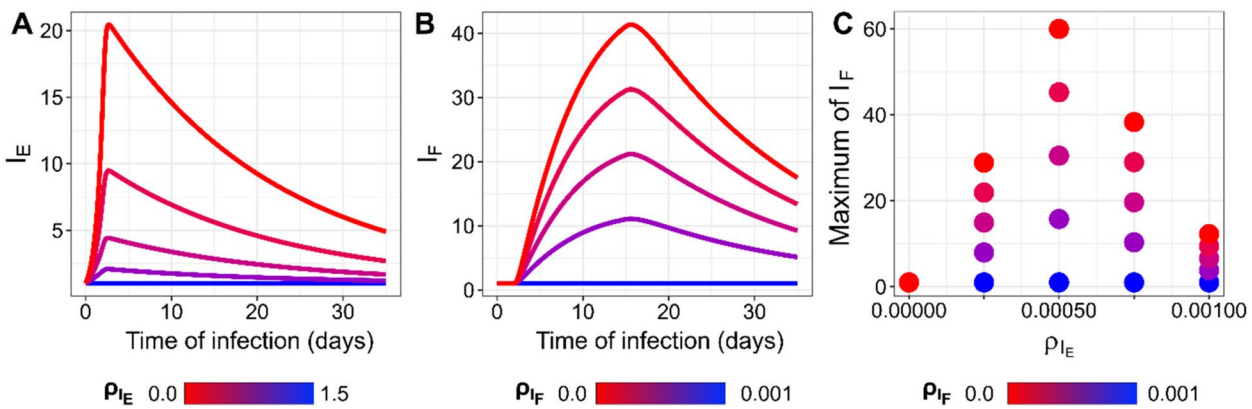

Fig. 4 Effect of replication rate on each immune response over the course of an infection. **A** effect of φ_{I_E} on I_E; **B** effect of φ_{I_F} on I_F, and **C** indirect effect of φ_{I_E} on I_F depending on φ_{I_F} with maximum I_F values observed during infection on the y-axis

where P followed a Gompertz growth, with a target amount of protein at maturity (P_m) and a growth rate parameter (β_P) estimated individually:

$$\frac{dP}{dt} = \beta_P \cdot \left(\frac{P}{P_m^{\alpha_{P_m}}}\right) \cdot log\left(\frac{P_m}{P}\right) \quad (18)$$

Wool was assumed to growth proportionally to P and was depleted when sheep were shorn.

$$\frac{dWool}{dt} = \beta_{Wool} \cdot P \quad (19)$$

Finally, the ratio between P and scaled mature protein ($P_m^{\alpha_{P_m}}$) determined the change in energy requirements for animal maintenance during its development:

$$E_{maint} = e_{maint} \cdot \left(\frac{P}{P_m^{\alpha_{P_m}}}\right) \quad (20)$$

Based on previous state variables P and L and on estimated FI, observed growth traits (BW and BFT) were defined as auxiliary variables with fixed parameters (specified in Table 1). Bodyweight was the sum of the different body components:

$$BW = P + L + Wool + Ash + Water + Gut\_Fill \quad (21)$$

with

$$Ash = \gamma_{Ash} \cdot P \quad (22)$$

$$Water = \gamma_{Water} \cdot P_m \cdot \left(\frac{P}{P_m}\right)^{\alpha_{Water}} \quad (23)$$

and

$$Gut\_Fill = FI \cdot \left(a_{Gut\_Fill} - b_{Gut\_Fill} \cdot MEC_{Feed}\right) \quad (24)$$

Back fat thickness was derived from a previous allometric equation [39], as follows:

$$BFT = exp\left(\frac{log(L) - a_{BFT} - b_{BFT} \cdot log(BW - Gut\_Fill)}{c_{BFT}}\right) \quad (25)$$

Parameter estimation

According to the model, observed differences in the above measurable performance and resistance traits are caused by individual differences in the genetic potentials for growth (protein and lipid deposition) and wool production, as well as in the immune responses. These can be represented by the model parameters $\theta = \left(P_m, L_m, \beta_P, \beta_{Wool}, \varphi_{I_E}, \varphi_{I_E}, HE_0\right)$ (Table 1). To account for individual variation in these latent model parameters θ, these parameter values associated with each individual were estimated from the data, together with the constant population-specific energy costs (e_{I_E} and e_{I_F}) associated with one unit of I_E and I_F respectively, in two main steps (Fig. 3).

Estimates for the individual parameters $\theta = (P_m, L_m, \beta_P, \beta_{Wool}, \varphi_{I_E}, \varphi_{I_F}, HE_0)$ were obtained as follows: the individual parameters related to growth (P_m, L_m, β_P, β_{Wool}) were estimated using data out-of-infection to describe the growth potential of each individual (step 1.1 in Fig. 3). The other individual parameters related to immunity (φ_{I_E}, φ_{I_F}) and the baseline level of HE (HE_0) were estimated using data during the infection period. For this last part, we assumed that values of growth parameters related to protein growth (P_m, β_{Wool}) were the same as out of infection, except the rate of protein synthesis β_P that may be affected by infection and was thus re-estimated together with φ_{I_E} and φ_{I_F} (step 1.2 in Fig. 3). When estimating the four parameters during the infection stage, we assumed fixed constant values of the immune energy costs (e_{I_E} and e_{I_F}) and other population specific parameters listed in Table 1.

Individual parameter estimates were obtained by minimizing differences between model predictions and data for that individual as outlined below. This procedure was then repeated for 100 different combinations of values for e_{I_E} and e_{I_F}, and the most likely values of e_{I_E} and e_{I_F} were then selected as those that minimise the differences between model predictions and data across all individuals (step 2 in Fig. 3).

Fitting criteria

Individual values for the parameters were estimated based on the minimization of a normalized residual sum of squares for each individual i ($NRSS_i$) defined as follows:

$$NRSS_i = \sum_{k=1}^{K}\left(\frac{\sum_{t=1}^{T_k}\left(\widehat{y}_{k,t,i} - y_{k,t,i}\right)^2}{SD(y_{k,i})}\right) \quad (26)$$

where $y_{k,t,i}$ and $\widehat{y}_{k,t,i}$ are the observed and predicted values, respectively, of trait k for individual i at time t. T_k is the last time-measurement for trait k, K is the number of measured traits and $SD(y_{k,i})$ is the standard deviation of trait k for individual i that is used to normalize each $RSS_{k,i}$. Note that each time-specific measurement of trait k is given the same weight when calculating the whole $NRSS_i$. When $SD(y_{k,i}) = 0$ (as it can be the case for *FEC* (log-transformed)) it was replaced by 1.

The predicted values $\widehat{y}_{k,t,i}$ were obtained using the host-parasite model with a given set of parameters θ. We searched for the set of parameters θ^* that minimize $NRSS_i$ using a modified version of the Levenberg–Marquardt

algorithm. This was implemented in R using the *nls.lm* function of the R-package *minpack.lm* [47].

The exact approach associated with the different steps is outlined below.

Step 1.1) estimation of individuals' growth parameters out-of-infection

In this step 1.1 (Fig. 3), observations for $K = 3$ traits (BW, BFT and $Wool$) were used to determine the values of the four parameters $\theta^* = (P_m, L_m, \beta_P, \beta_{Wool})$ that minimize the corresponding $NRSS_i$. A mentioned earlier, a central model assumption was that growth was driven by protein accretion to reach a genetically determined target value at maturity P_m. However this value could not be estimated reliably during the infection as the corresponding growth period was relatively short and feeding conditions were very favorable to fattening (i.e. concentrate ad libitum) compared with the periods where animals were uninfected (forage and concentrate to meet animal requirements). In this first step we thus aimed to estimate P_m using growth data before and after the experimental period to capture the 'normal' growth pattern before reproduction (Fig. 5A). For this we used the empirical growth equation (Eq. (18)). In addition to P_m we also estimated the 'normal' protein growth rate parameter β_P even though we considered that this parameter could vary during infection (cf. next subsection). Based on BFT and $Wool$ measurements it was possible to separate P_m from other BW components at maturity (following Eqs. (21–25)). Data on BFT (Fig. 5B) was informative of the level of lipid. However, as food intake was not recorded out of the infection lipid deposition could not be calculated based on EB during those periods (as shown in Eq. (14)). Instead a 'normal' lipid growth was assumed to follow a sigmoid pattern as proposed in [33]. This pattern is driven by $\frac{dP}{dt}$ as follows:

$$\frac{dL}{dt} = \frac{dP}{dt} \cdot \frac{L_m}{P_m} \cdot d \cdot \left(\frac{P}{P_m}\right)^{d-1} \quad (27)$$

where the estimated parameter L_m represents the level of L at maturity.

Based on fleece weight recorded after the experimental period (Fig. 5A), we could also estimate the individual wool growth parameter β_{Wool} of Eq. (19). Finally, in Eq. (21) all other BW components than P, L and $Wool$ were simply derived from P, assuming equal parameter values among individuals.

Step 1.2) estimation of individual parameters during infection for fixed values of immune energy costs

During the infection we first used the model of within-host parasite dynamic to estimate the baseline level of HE (HE_0). Values of HE_0 were thus logically assumed to be independent of the energy cost of infection. Then, the two coupled sub-models (i.e. the host-parasite system and the host energy budget were used to estimate parameters φ_{I_E} and φ_{I_F} that set the magnitude of the two immune responses. For the energy budget sub-model, we used the values of P_m and β_{Wool} estimated out-of-infection (see previous sub-section) whereas we re-estimated β_P (β_P^*) considering that the protein growth rate (but not the target P_m) could deviate from the normal value estimated out-of-infection. In this step 1.2 (Fig. 3), lipid deposition was calculated based on food intake (Eq. (14)) so the parameter L_m was no longer needed. All other parameters related to immune responses were assumed equal among-individuals, including e_{I_E} and e_{I_F}. Thus, for each individual i the values of the parameters (φ_{I_E}, φ_{I_F}

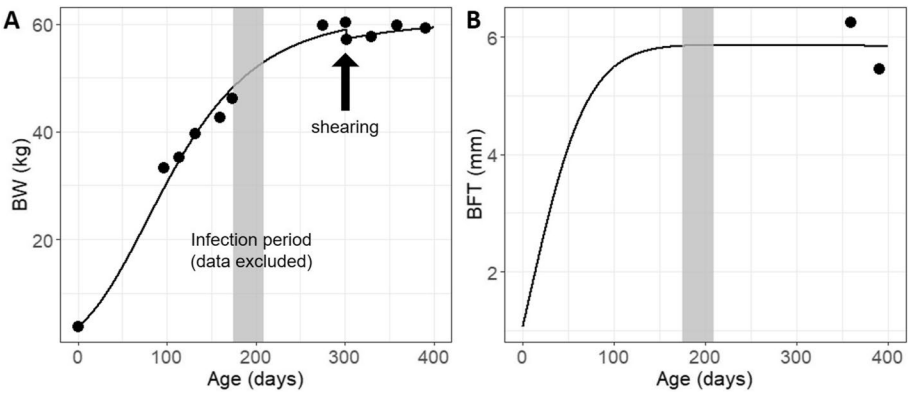

Fig. 5 Example of individual growth curve fitting to estimate protein weight at maturity based data observed out of infection. **A** data on body weight (*BW*) and **B** back fat thickness ($_{BFT}$) were used. Points and lines represent observed data and model predictions, respectively. Note the drop in body weight at shearing that was used to estimate wool growth. Data observed during the infection period (grey area) were not used for model fitting in this step. See S2 Fig for all 42 individuals (Animal n°20000188131 represented here)

and β_P*), were determined that minimize the individual's $NRSS_i$ comprising $K = 4$ traits (FEC, HE, BW, BFT).

Step 2) estimating the immune energy costs e_{I_E} and e_{I_F}

Estimates of individuals' immune parameters following the procedure outlined in 3.3.1 were obtained for 100 (10 × 10) different combinations of values of e_{I_E} and e_{I_F} (step 2; Fig. 3). These combinations comprised 10 different values of e_{I_E} and e_{I_F}, respectively (within the range [0; 0.09] and [0; 0.021]; for e_{I_E} and e_{I_F} respectively, with 10 equal increments within each case). This grid was obtained by refining a first grid exploration on larger ranges to focus on values of $NRSS_i$ below 17 (which explains the different maximum values for e_{I_E} and e_{I_F}). For each combination, *NRSS* calculated during the infection (with $K = 4$ traits) was averaged over all individuals from both lines. The most likely combination of e_{I_E} and e_{I_F} was then considered as the one that minimizes the average $NRSS$.

Results

Immune energy costs and trade-off between host resistance and fat storage

Consistent with H1, the positive relationship that we observed among individuals between host resistance (FEC) and storage (BFT) (Fig. 6A) was better predicted assuming positive values of immune energy costs (e_{I_E} and e_{I_F}) than assuming zero immune energy costs (Fig. 6B). In other words, a higher dynamic immune response in R vs. S sheep contributed to the observed differences between lines both in terms of host resistance and in terms of fat reserves (Fig. 6). This difference in immune responses led to an energy allocation $E_{immunity}$ that was about three times larger on average in R vs. S sheep (Fig. 7), which effectively translated into a large difference in resistance to parasites (means of maximum predicted *FEC* based on negative binomial regression = 49 and 1,223 eggs/g in R and S sheep, respectively). In contrast, since energy intake was the same under H0 and H1, then more energy was available for growth and body reserves when zero

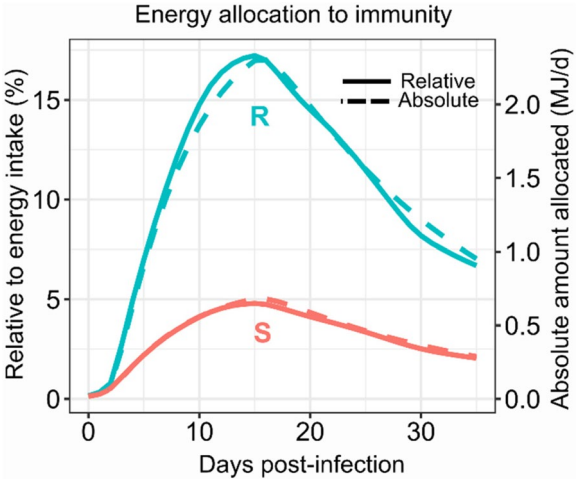

Fig. 7 Average energy allocation to immunity predicted during infection with *Haemonchus contortus* in individuals from resistant (R) and susceptible (S) lines. Energy allocation is expressed relatively to energy intake and absolutely as the amount allocated

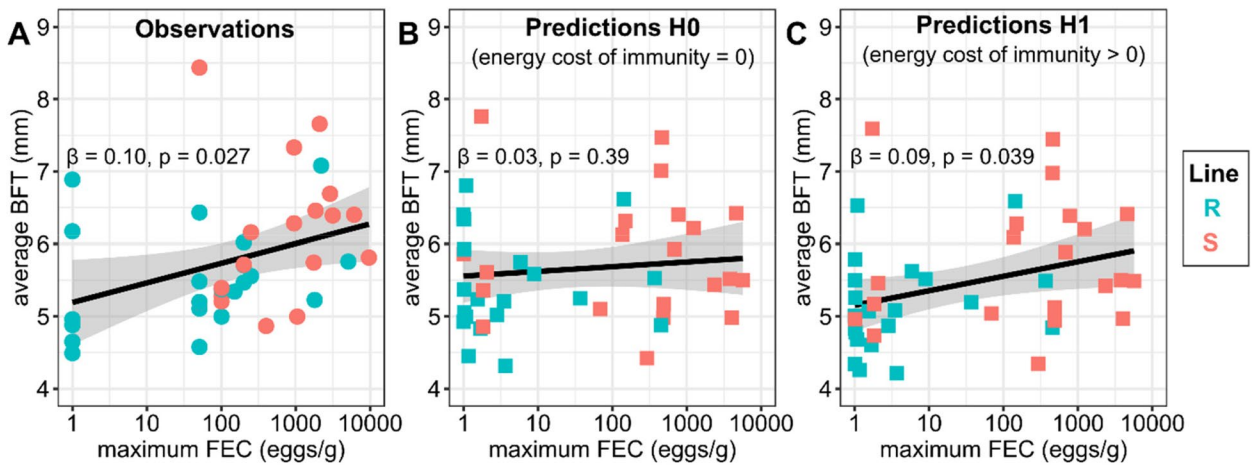

Fig. 6 Relationship among individuals from resistant (R) and susceptible (S) lines between host resistance and fat reserves observed (A) and predicted assuming zero (H0; B) or positive immune energy cost (H1; C). **A** Observed data (points) supports a trade-off between host resistance (approximated by maximum fecal egg count (FEC)) and fat reserves (approximated by average back fat thickness (BFT)). **B** Individual model predictions (squares) under hypothesis H0 do not lead to the observed trade-off, **C** contrary to predictions under H1. Solid line and grey areas represent linear regression lines with their prediction interval. Regression coefficients (β) are indicated with their level of significance. Note that the scale of x-axis is log-transformed to account for the skewed distribution of *FEC*

immune energy costs were assumed (H0). In this case, the model tended to overestimate *BFT* in R sheep and the trade-off between *BFT* gain and host resistance did not occur (Fig. 6B).

Evidence for positive immune energy costs

The optimal values of immune energy costs in support of H_1 corresponded to the best average model fit across the 42 individuals. This optimum was obtained when both immunity against parasite establishment (I_E) and against parasite fecundity (I_F) entailed small, yet positive energy costs (i.e. $e_{I_E} = 0.01$ and $e_{I_F} = 0.0072$; Fig. 8). Compared with the scenario H0, positive values for e_{I_E} and e_{I_F} improved the goodness of fit on average (mean normalized residual sum of square $NRSS = 14.54$ (H0) vs. 12.97 (H1)) as well the prediction accuracy (SD $NRSS = 7.04$ (H0) vs. 4.73 (H1)). However this improvement varied between lines. In general, *NRSS* was not as low in R sheep as in S sheep mainly due to the zero-inflated distribution of *FEC* in the R line that made this trait more difficult to predict, regardless the energy constraint (H0: $NRSS_R = 16.84$ vs. $NRSS_S = 12.24$; $t_{(40)} = 2.22$, $p = 0.032$). However under H1 the better prediction of BFT in R sheep mainly contributed to a large *NRSS* improvement in this line so that the difference in goodness of fit was much reduced between lines (H_1: $NRSS_R = 14.32$ vs. $NRSS_S = 11.61$; $t_{(40)} = 1.91$, $p = 0.06$).

Results of individual model fitting show that the four different trait dynamics are relatively well predicted at the individual level, as illustrated by two representative individuals of each line (Fig. 9; R sheep $NRSS = 15.8$; S sheep: $NRSS = 14.6$). Observed responses and model fits for all 42 animals are provided in S3 Fig and individual model errors in S4 Fig. As would be expected, the model captured the overall trends but not all nuances observed in the experimental data. For instance, small *FEC* values

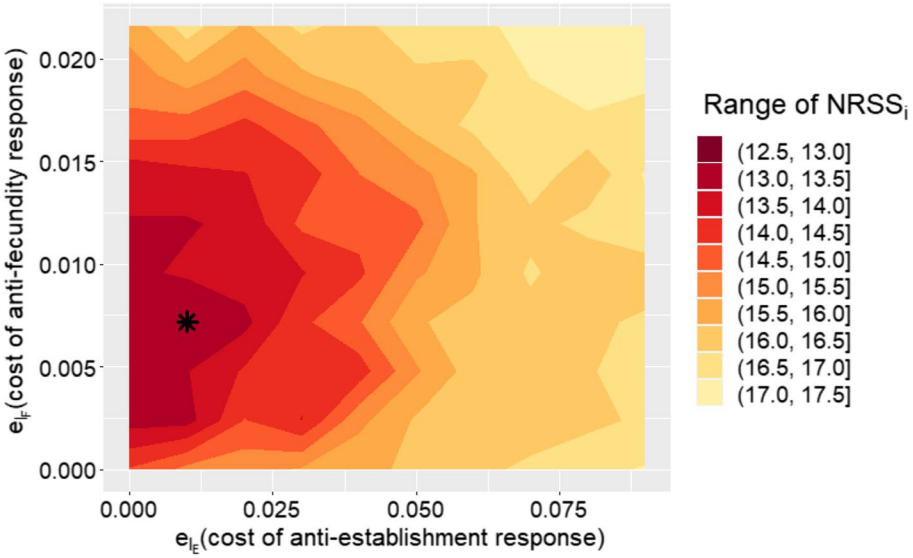

Fig. 8 Model goodness of fit according to the assumed values for the energy cost of two immune responses against *Haemonchus contortus*. Parameters e_{I_E} and e_{I_F} refer to the energy cost of immunes responses against larvae establishment (I_E) and fecundity (I_F), respectively. The fitting criteria used for parameter estimation was the normalized residual sum of squares for each individual i ($NRSS_i$). The average *NRSS* over the 42 individuals is represented. The global optimum is indicated with an asterisk

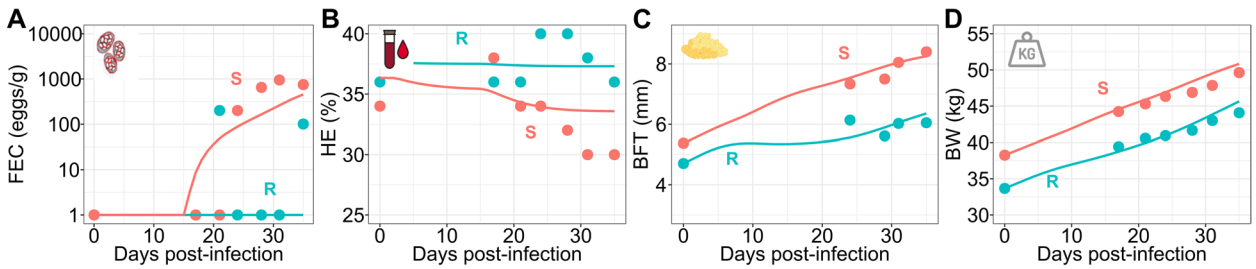

Fig. 9 Individual model fit for two representative sheep of lines selected for resistance (R) or susceptibility (S) to *Haemonchus contortus*. Individual model observations (points) and model predictions under H1 (solid lines). *FEC* = parasite fecal egg count; *HE* = blood haematocrit; *BFT* = backfat thickness; *BW* = body weight. Note that in (A) the scale of y-axis is log-transformed to account for the skewed distribution of *FEC*

of individuals with zero FEC during most of the infection time were not well predicted (Fig. 9A).

Evidence for differences in immunity between lines

The immune energy cost assumption differently affected the estimates for the three host parameters related to immunity (φ_{I_E} and φ_{I_F}) and to protein growth (β_P^*) during infection. In line with expectation *iv*, higher replication rates φ_{I_E} and φ_{I_F} led to stronger immune responses I_E and I_F, in the R *vs* S line, independent of whether energy costs apply or not (Table 2). In contrast, the average estimates of β_P^* decreased in both lines under H1, with relatively stronger reductions in the R line. Baseline values HE_0 were not different between lines (R = 34.8 vs. S = 35.4; $t_{(40)} = -0.75$, $p = 0.43$). Contrary to H0, under H1 energy can be allocated to immunity at the expense of body growth and reserves. This energy reallocation was supported, mainly in R sheep, so that similar estimates for β_P^* were obtained between lines when costly resistance was assumed during infection (Table 2). Accordingly, the observed data did not support any difference in BW between infected lines (Fig. 1Aiii).

No differences in growth and energy storage between lines out-of-infection

Prior to the parameter estimation during the infection, growth trajectories including four individual parameters were fitted to BW, BFT and $Wool$ data observed out-of-infection (Table 3). Protein weight at maturity (P_m) and wool growth rate (β_{Wool}) were assumed to be unaffected by infection and were thus used in the previous fitting results whereas protein growth rate (β_P) was re-estimated during infection (Table 2) and lipid weight at maturity (L_m) was not re-used (as body lipid and its proxy (BFT) were predicted from the model of energy budget during infection).

We did not detect any difference between the two selection lines among the four growth parameters estimated out of infection (Table 3). This confirmed our expectation (v) that sheep from the two selection lines diverged in their immune parameter values (φ_{I_E}, φ_{I_F}), but not in their growth or wool production parameters as host selection was on resistance only. In addition, the values of β_P were close to the interspecific estimate (in sheep and cattle; 0.02335 $kg^{0.27}$/day) found by [33]). Those values of β_P were higher than those estimated during the infection period (β_P^* around 0.014–0.018; Table 2). However we found that β_P and β_P^* were uncorrelated (see S1 Fig representing correlation between all parameters), thus suggesting that infection-induced immunity may mediate growth. In particular, β_P tended to correlate negatively with immune parameters φ_{I_E} ($r = -0.38$, $t_{(40)} = -0.3$, $p = 0.01$) and φ_{I_F} ($r = -0.29$, $t_{(40)} = -0.191$, $p = 0.06$), in support of stronger immune responses deployed by slow-growing lambs compared with fast-growing ones.

Table 3 Mean (with standard deviation) of growth parameters estimated out of infection in sheep from lines selected on resistance (R) or susceptibility (S) to *Haemonchus contortus*

Parameter [a]	Line R ($n = 21$)	Line S ($n = 21$)	$t_{(df=40)}$ [b]	p
P_m	6.88 (0.364)	6.75 (0.433)	1.027	0.31
L_m	15.08 (2.033)	15.55 (2.602)	−0.641	0.53
β_P	0.0224 (0.0025)	0.0239 (0.0037)	−1.551	0.13
β_{Wool}	$11{\cdot}10^{-5}$ ($3.5{\cdot}10^{-5}$)	12.10^{-5} ($2.7{\cdot}10^{-5}$)	−0.518	0.61

[a] P_m = protein weight at maturity; L_m = lipid weight at maturity; β_P = Protein growth rate estimated out-of-infection; β_{Wool} = Wool growth rate

[b] Lines differences were tested based on unpaired t-test

Discussion

Host resistance to helminth infections typically relies on an adaptive T helper 2 (Th2) cell response, which involves a myriad of energy-demanding processes [48, 49]. Upon activation, immune response may then contribute to elevate host metabolism. Yet, quantifying the energy allocated to immunity remains a long-standing challenge to link the physiological costs of host defenses to their evolution [6, 26], and thereby to develop an

Table 2 Impact of assumption on immune energy costs on mean values of immunity and growth parameters estimated during infection in sheep from lines selected on resistance (R) or susceptibility (S) to *Haemonchus contortus*

Parameter[a]	H0: zero immune energy costs				H1: positive energy costs			
	Line R ($n = 21$)	Line S ($n = 21$)	$t_{(df=40)}$ [b]	p	Line R ($n = 21$)	Line S ($n = 21$)	$t_{(df=40)}$ [b]	p
φ_{I_E}	1.336	0.950	2.44	0.019	1.184	0.967	3.95	< 0.001
φ_{I_F}	−5.291	−7.369	4.56	< 0.001	−5.114	−7.294	4.74	< 0.001
β_P^*	0.0185	0.0154	1.4	0.17	0.0141	0.0143	−0.104	0.92

[a] φ_{I_E} = replication rate of immunity against parasite establishment; φ_{I_F} = replication rate of immunity against parasite fecundity; β_P^* = Protein growth rate estimated during the infection

[b] Lines differences were tested based on unpaired t-test

evolutionary perspective on immunometabolism [2]. In most host-parasite systems, limited knowledge of immuno-metabolism mechanisms conferring host resistance proscribes any attempt to deduce specific immune energy costs using an analytical approach. Conversely, costs can be inferred at the level of the whole organism if the overall energy budget and changes in energy reallocation between immunity and other processes can be depicted over the course of infection [25]. By fitting dynamic mechanistic models of energy allocation to existing data, we estimated an induced energy cost of resistance in divergent host genotypes (Q1), and thereby lay the groundwork for establishing a link between host energy allocation and the emergence of among-individual trade-offs (Q2). Below we discuss the features of the energy cost of resistance that we found, the way it was inferred and its links with a trade-off among individuals of selected lines in our model system.

In agreement with previous estimates for immune costs mostly ranging from 5 to 15% of metabolic rate in various host–pathogen systems [26], the induced immune energy cost found in this study was low to moderate in magnitude. Still, helminth parasite infections incur substantial costs on mammals' metabolism [50, 51]. Meta-analyses in sheep have quantified large impacts on lamb body weight ([52]) or metabolizable energy requirements ([53]). However, those large effects mainly occur during the prolonged acute phase of infection [54], directly as a result of highly pathogenic nematodes such as *H. contortus*. This latter phase was abbreviated in our experiment by drenching at five weeks of infection, which may explain the lack of difference in final body weight between lines. As our infectious challenge was originally designed to evaluate future breeding animals [55], it was short enough to minimize the direct infection costs that could impair hosts' reproductive potential. Our results thus coincide with previous evidence of relatively low resistance costs, mostly paid over a few days during the prepatent phase [56]. Accordingly, sheep resistance to helminth infections has been viewed as a short-term diversion of host resources providing a long-term advantage on the avoidance of parasitological consequences [54].

So far, there have been few attempts to measure the energy cost of host resistance from real data. In general, attempts based on the sole measurement of resting metabolic rate have been considered too simplistic to capture the specific contribution of immune processes in the whole energy budget [23]. In livestock, several studies have relied on feed efficiency estimations [54, 57]. Those are usually based on multiple linear regression of host feed intake against host traits associated to main energy sinks (e.g. body weight gain), as well parasite burden (FEC). A lower energy efficiency of production in infected animals would support an overall infection cost. The immune contribution to this cost can then be estimated by comparing feed efficiency between resistant animals and others. For instance, sheep selected for resistance to helminths required about 4% more energy per day relative to control animals during an infectious challenge with two helminths (*Trichostrongylus colubriformis* and *Ostertagia circumcincta*) [57]. However, estimates based on linear regression techniques applied to feed efficiency may provide poor estimates of the true resistance costs given their ignorance of host-parasite interactions over time. In particular, nutritional effects on host resistance taking place early in the infection can be difficult to assess since most infection traits used as covariate only vary after the prepatent period (e.g. FEC, HE). Moreover, transient changes in nutrients use make the requirement of host resistance particularly challenging to detect insofar as effects on animal performances may be subtle or compensated for by the end of the infection period [56, 57]. In our case, although resistant animals were found to allocate up to 15% of their ME intake towards immune response against *H. contortus* at two weeks of infection, this energy allocation was halved three weeks later, when the peak of parasite egg excretion is usually observed for this parasite species. The modelling approach proposed here thus accounts for important methodological difficulties to link animal feed intake to dynamic host-parasite interaction. Although many mechanistic models of host-parasite interaction have been previously developed, most of them ignored the cost of host resistance (e.g. in bioenergetics models in ecology [58]) or at best assumed it but never estimated it based on observed data (e.g. in livestock models of helminth infections [39, 59–61]).

Besides the limitations due to the single dataset we used to calibrate our model, some model assumptions are important to point out to help interpreting the significance of the estimated host resistance costs. In particular, we assumed that host energy balance was fully buffered by body lipid reserves (Eq. 14). This may not necessarily occur as animals may also defend a certain level of body fatness and therefore adjust their energy allocation between protein growth and immunity accordingly [3]. As previously assumed [44], protein growth and immunity were given higher nutritional priority over changes in body lipid in our model. Yet more complex allocation rules could be considered [62], which may notably lead to different trade-off expressions according to the diet energy density.

While dietary nutrient availability is usually considered as the main limiting factor to explain the occurrence of resource allocation trade-off during parasite infections, trade-offs can also occur in nutrient-rich environments as a result of parasite-induced anorexia [63]. Anorexia may be a pathological consequence of parasitism, or on the contrary, an adaptive host response to cope with the infection [11]. Our model did not incorporate any assumption in this respect; instead individual feed intake data automatically recorded was used as an independent model input. Thus, when considering the different patterns of feed intake between lines (Fig. 1Av) without assuming an energy cost of host resistance in the model (H0), the simulated difference in BFT between the lines was still maintained, albeit only at 50% compared with the scenario of costly resistance (H1). This thus supports the view that reduced feed intake together with energy reallocation are major contributors of reduced performance in parasitized sheep [64]. Therefore the coordinated changes in those two aspects may well be part of an effective host response to infection [11].

The incorporation of acquired immunity during the course of infection remains an important challenge for the development of mathematical models of host-parasite interaction in vertebrates [65]. In general, acquired immunity cannot be modelled explicitly, except for a few host-parasite systems where biomarkers of parasite-specific immunity associated with host resistance have been recognized (e.g. immunoglobulins E and A against *Teladorsagia circumcincta* [66]). Instead, host-parasite interaction models of helminth infections have often considered parasite specific immunity as a single latent, unobserved variable that is acquired proportionally to the cumulated exposure (intake) of infective larvae. Based on the same notion of virtual immune response, our model differs from previous approaches in two aspects: first, it focuses on the acquisition of immunity during the development of a single cohort of parasites (i.e. single-dose infection) rather than across successive infections; second it represents several immune variables affecting a particular aspect of the parasite development rather than a single immune variable affecting all aspects. This approach remains incomplete as for example, two of the three main host effects on the parasite dynamics [36] were included in our model (i.e. establishment, fecundity) whereas the effects on adult parasites mortality occurring mainly during late infection could not be explored with our short-term challenge. Including a host effect on parasite mortality in the model would require a third immune variable ("I_M") with additional parameters to be estimated. This perspective further extends the view presented here that multiple strategies of host resistance with varying degree of energy efficiency could be expressed as a result of multiple immune responses with their specific energy costs. Consequently, representing the acquisition of each immune response across successive infections would not only be relevant to represent situations of repeated infections closer to natural infections, but also to explore the long-term consequences of various strategies of host resistance in terms of energy efficiency.

Currently, the links between evolutionary (genetic) trade-offs and the demands and physiological control of energy for immunity and other functions during a host's lifetime are still largely unknown [20, 67, 68]. According to the allocation hypothesis, the energy cost of immunity should be large enough to impair host fitness, and consequently limit selection for host resistance to pathogens [7, 69–71]. Based on our findings, there are only a few reasons to expect energy allocation constraints to directly shape the outcomes of selection for sheep resistance, as usually assumed [3, 4]. If large resistance costs actually exist this would mean that some important cost components were left unaccounted for in our approach (e.g. long-lasting effects of immunopathology). The relatively small and transient energy cost of resistance that we found could otherwise possibly lead to significant impacts on fitness if animals were evolving in conditions that strongly constrict their energy budgets (e.g. exposure to feed shortage, supplementary energy-demanding activities). Still, our observation an energetic trade-off in ad libitum feeding conditions suggests that causes other than energy scarcity can lead to trade-offs in the evolution of host defenses.

Among other potential causes of trade-offs, obligate genetic antagonisms (e.g. due to pleiotropy [72]) can occur between host defenses and growth. Such trade-offs are usually considered as constitutive and should thus result in different growth between lines regardless of infection [67]. For instance, a relationship between growth and host resistance may exist if immunity to helminths develops at a certain degree of maturity relative to adult body weight [73]. In our study, we found similar growth parameters among lines out of infection (Table 3), although this finding is based on a critical assumption that infection did not affect growth patterns post-infection. Assessing the growth patterns of our lines in the absence of any infection is thus needed to confirm our results. However, we found that relative growth rate was negatively related to the strength of immune responses in both resistant and susceptible sheep. Likewise, intense livestock selection for fast growth commonly leads to increased diseases susceptibility [3] whereas the reciprocal consequences of selection for

resistance on growth are more ambiguous [68]. Such outcomes likely illustrate complex interferences between growth, development and the immune system [69]. In particular, pleiotropy in energy metabolism and immune signaling pathways is increasingly seen as a key mechanism promoting the evolution of immune costs induced by infection [70].

Irrespective of their proximate causation, the existence of transient costs of host defenses should be a condition *sine qua non* for the evolution of induced immunity. If immunity conferring host resistance was cost-free it could be constantly deployed and induction would be pointless [71]. On the other hand, if moderate energy costs of host resistance (as found here) were constantly paid, cumulated costs would likely be too large to be sustained over lifetime. Despite this rationale, few studies have actually shown genetic variation in induced costs [74, 75]. Preliminary evidence that we showed in this study relates to induced energy cost of host resistance between selected lines. Still a note of caution is due here concerning the genetic nature of the trade-off that we observed among our selected lines. Indeed, other processes than a trade-off may have led to a difference in fat storage between lines (e.g. founder effects and/or genetic drift). More robust evidence would require to replicate our selection experiment although this is particularly long and costly in a large vertebrate host [76]. If sample size was sufficiently large to reliably estimate variance components, genetic variation could also be further explored using the inference approach presented in this study within line or combined with a quantitative genetic design at a population scale. In populations evolving resistance, induced immunity may be a first step for the evolution of a constitutive immunity, that is a genetically hard-wired trait constitutively expressed even under non-infectious conditions [77, 78]. Perhaps this evolution in hosts defenses also gears towards alternative physiological regulatory networks of the immune system and other physiological systems, that are energetically more efficient [79, 80].

Conclusion

In summary, this study inferred a small and transient induced energy cost of resistance to parasites in selected lines of a vertebrate host. Our results thus highlight how selection on host resistance may lead to trade-offs due to energy reallocation during infection and despite low energetic constraints. This is a first step to bridge two long-standing issues in the evolution of host defenses, namely to quantify the energy costs of immunity and to assess genetic trade-off between host defenses and other fitness components. Integrating those issues is key to address the link between immune energy costs and evolutionary trade-offs that is abstractly pictured in the energy allocation hypothesis [78]. Building on our approach, combining mathematical models of host-parasite interactions and experiments offers new perspectives to scale up the consequences of within-host dynamics (as envisioned in insects systems [81]), particularly to explain and predict the role of energy allocation trade-offs in the evolution of host defenses.

Supplementary Information

The online version contains supplementary material available at https://doi.org/10.1186/s12862-024-02340-0.

Supplementary Material 1. S1 Fig. Values of the 7 individual parameters estimated out of infection and during infection in the 42 sheep from lines selected on resistance (R) ($n = 21$) or susceptibility (S) ($n = 21$) to *Haemonchus contortus*. Parameter estimated during infection: φ_{IE} ("rhol_E") = replication rate of immunity against parasite establishment; φ_{IF} ("rhol_F") = replication rate of immunity against parasite fecundity; β_P^* ("B_Protein_inf") = Protein growth rate estimated during the infection. Note that φ_{IF} was log-transformed to reduce distribution skewness. Parameter values during infection are those obtained for the optimum energy costs assumed under H_1 (i.e. $e_{IE} = 0.01$ and $e_{IF} = 0.0072$). Parameter estimated out-of-infection: P_m ("Protein_m") = protein weight at maturity; L_m ("Lipid_m")= lipid weight at maturity; β_P ("B_Protein_out")= Protein growth rate estimated out-of-infection; β_{Wool} ("K_Wool")= Wool growth rate.

Supplementary Material 2. S2 Fig. Individual growth curve fitting to estimate protein weight at maturity based data observed out of infection in the 42 sheep from lines selected on resistance (R) ($n = 21$) or susceptibility (S) ($n = 21$) to *Haemonchus contortus*. For each animal (A) data on body weight (BW) and (B) back fat thickness (BFT) were used. Points and lines represent observed data and model predictions, respectively. Note the drop in body weight at shearing that was used to estimate wool growth. Data observed during the infection period (grey area) were not used for model fitting in this step.

Supplementary Material 3. S3 Fig. Individual model fit for the 42 sheep of lines selected for resistance ($n = 21$) or susceptibility ($n = 21$) to *Haemonchus contortus* assuming immune energy costs or not in the model. Points represent observed data, solid lines are model predictions for the optimum energy costs assumed under H_1 (i.e. $e_{IE} = 0.01$ and $e_{IF} = 0.0072$), dashed lines are model predictions under H_0 when no energy costs for host resistance are assumed (i.e. $e_{IE} = 0$ and $e_{IF} = 0$). FEC = parasite fecal egg count; HE = blood haematocrit; BFT = backfat thickness; BW = body weight.

Supplementary Material 4. S4 Fig. Distribution of within-individual model errors for the 42 sheep of lines selected for resistance (R) or susceptibility (S) to *Haemonchus contortus*. Model errors are calculated as the difference between model predictions and observations. The two individuals plotted in Fig 9 in the main text are highlighted. (A) FEC = parasite fecal egg count; (B) HE = blood haematocrit; (C) BFT = backfat thickness; (D) BW = body weight. Note that in (A) FEC is log-transformed to account for its skewed distribution.

Acknowledgements

We pay tribute to the memory of our colleague and friend Carole Moreno-Romieux who passed away in June 2022.

Authors' contributions

FD, CMR and ABDW participated to the design of the work. FD and CMR contributed to data acquisition. FD and ABDW analysed and interpreted data. FD developed, implemented and run the mathematical model. FD drafted the

work and revised it with ABDW. All authors have agreed both to be personally accountable for the author's own contributions and to ensure that questions related to the accuracy or integrity of any part of the work, even ones in which the author was not personally involved, are appropriately investigated, resolved, and the resolution documented in the literature.

Funding
The work was funded by the projects SusTradeOff (ERA-NET SUSAN, no 696231) and SMARTER (H2020, no 772787). ADWs contribution is also partly funded by the BBSRC Institute Strategic Program Grants BBS/E/D/20002172&/30002275 and BBS/E/RL/230002A & /230002D.

Data availability
The observed data, model code, parameter values and model outputs can be accessed through https://doi.org/10.6084/m9.figshare.25323595 (https://figshare.com/s/2579a566cefbb48487aa).

Declarations

Ethics approval and consent to participate
The experimental procedures to produce data used in this work were approved by the French Ministry for Higher Education and Research and the Centre Val de Loire ethics committee under the experimental approval D18-174–01.

Consent for publication
Not applicable.

Competing interests
The authors declare no competing interests.

Received: 18 September 2024 Accepted: 16 December 2024
Published online: 28 January 2025

References

1. Sadd BM, Schmid-Hempel P. Principles of ecological immunology. Evol Appl. 2009;2:113–21.
2. Wang A, Luan HH, Medzhitov R. An evolutionary perspective on immunometabolism. Science. 2019;363:eaar3932.
3. Rauw WM. Immune response from a resource allocation perspective. Front Gene. 2012;3:267.
4. Sheldon BC, Verhulst S. Ecological immunology: costly parasite defences and trade-offs in evolutionary ecology. Trends Ecol Evol. 1996;11:317–21.
5. Zuk M, Stoehr AM. Immune Defense and Host Life History. Am Nat. 2002;160:S9–22.
6. Demas GE, Greives T, Chester E, French S. The energetics of immunity. In: Demas GE, Nelson RJ, editors. Ecoimmunology. New York: Oxford University Press; 2012. p. 259–96.
7. Lochmiller RL, Deerenberg C. Trade-offs in evolutionary immunology: just what is the cost of immunity? Oikos. 2000;88:87–98.
8. Delmastro-Greenwood MM, Piganelli JD. Changing the energy of an immune response. Am J Clin Exp Immunol. 2013;2:30–54.
9. Schwenke RA, Lazzaro BP, Wolfner MF. Reproduction-Immunity Trade-Offs in Insects. Annu Rev Entomol. 2016;61:239–56.
10. Colditz IG. Effects of the immune system on metabolism: implications for production and disease resistance in livestock. Livest Prod Sci. 2002;75:257–68.
11. Kyriazakis I, Tolkamp BJ, Hutchings MR. Towards a functional explanation for the occurrence of anorexia during parasitic infections. Anim Behav. 1998;56:265–74.
12. Ganeshan K, Nikkanen J, Man K, Leong YA, Sogawa Y, Maschek JA, et al. Energetic trade-offs and hypometabolic states promote disease tolerance. Cell. 2019;177:399–413.e12.
13. Mucha S, Tortereau F, Doeschl-Wilson A, Rupp R, Conington J. Meta-analysis of genetic parameters for resilience and efficiency traits in goats and sheep. Animal. 2022;16:100456.
14. Gold S, Regan CE, McLoughlin PD, Gilleard JS, Wilson AJ, Poissant J. Quantitative genetics of gastrointestinal strongyle burden and associated body condition in feral horses. Int J Parasitol: Par Wildlife. 2019;9:104–11.
15. Hayward AD. Genetic parameters for resistance to gastrointestinal nematodes in sheep: a meta-analysis. Int J Parasitol. 2022;52:843–53.
16. Auld SKJR, Penczykowski RM, Housley Ochs J, Grippi DC, Hall SR, Duffy MA. Variation in costs of parasite resistance among natural host populations. J Evol Biol. 2013;26:2479–86.
17. Labbé P, Vale PF, Little TJ. Successfully resisting a pathogen is rarely costly in *Daphnia magna*. BMC Evol Biol. 2010;10:355.
18. Penley MJ, Greenberg AB, Khalid A, Namburar SR, Morran LT. No measurable fitness cost to experimentally evolved host defence in the *Caenorhabditis elegans-Serratia marcescens* host-parasite system. J Evol Biol. 2018;31:1976–81.
19. Rigby MC, Hechinger RF, Stevens L. Why should parasite resistance be costly? Trends Parasitol. 2002;18:116–20.
20. Schmid-Hempel P. Variation in immune defence as a question of evolutionary ecology. Proc R Soc Lond B. 2003;270:357–66.
21. Ardia DR, Gantz JE, Brent C, Schneider, Strebel S. Costs of immunity in insects: an induced immune response increases metabolic rate and decreases antimicrobial activity. Funct Ecol. 2012;26:732–9.
22. Martin LB, Weil ZM, Nelson RJ. Seasonal changes in vertebrate immune activity: mediation by physiological trade-offs. Phil Trans R Soc B. 2008;363:321–39.
23. Robar N, Murray DL, Burness G. Effects of parasites on host energy expenditure: the resting metabolic rate stalemate. Can J Zool. 2011;89:1146–55.
24. Hite JL, Pfenning AC, Cressler CE. Starving the enemy? Feeding behavior shapes host-parasite interactions. Trends Ecol Evol. 2020;35:68–80.
25. Bashir-Tanoli S, Tinsley MC. Immune response costs are associated with changes in resource acquisition and not resource reallocation. Funct Ecol. 2014;28:1011–9.
26. Hasselquist D, Nilsson J-Å. Physiological mechanisms mediating costs of immune responses: what can we learn from studies of birds? Anim Behav. 2012;83:1303–12.
27. Hall MD, Phillips BL, White CR, Marshall DJ. The hidden costs of resistance: contrasting the energetics of successfully and unsuccessfully fighting infection. Funct Ecol. 2024;38:714–23.
28. McRae KM, Stear MJ, Good B, Keane OM. The host immune response to gastrointestinal nematode infection in sheep. Parasite Immunol. 2015;37:605–13.
29. Hendawy SHM. Immunity to gastrointestinal nematodes in ruminants: effector cell mechanisms and cytokines. J Parasit Dis. 2018;42:471–82.
30. Alba-Hurtado F, Muñoz-Guzmán MA. Immune responses associated with resistance to haemonchosis in sheep. Biomed Res Int. 2013;2013:1–11.
31. Sallé G, Deiss V, Marquis C, Tosser-Klopp G, Cortet J, Serreau D, et al. Genetic × environment variation in sheep lines bred for divergent resistance to strongyle infection. Evol Appl. 2021;14:2591–602.
32. Douhard F, Doeschl-Wilson AB, Corbishley A, Hayward AD, Marcon D, Weisbecker J, et al. The cost of host genetic resistance on body condition: evidence from divergently selected sheep. Evol Appl. 2022;15:1374–89.
33. Emmans GC. A method to predict the food intake of domestic animals from birth to maturity as a function of time. J Theor Biol. 1997;186:189–99.
34. Sallé G, Jacquiet P, Gruner L, Cortet J, Sauvé C, Prévot F, et al. A genome scan for QTL affecting resistance to *Haemonchus contortus* in sheep. J Anim Sci. 2012;90:4690–705.
35. Smith G. The population biology of the parasitic stages of *Haemonchus contortus*. Parasitology. 1988;96:185–95.
36. Saccareau M, Sallé G, Robert-Granié C, Duchemin T, Jacquiet P, Blanchard A, et al. Meta-analysis of the parasitic phase traits of *Haemonchus contortus* infection in sheep. Parasit Vectors. 2017;10:201.
37. Dargie JD, Allonby EW. Pathophysiology of single and challenge infections of *Haemonchus contortus* in Merino sheep: studies on red cell kinetics and the "self-cure" phenomenon. Int J Parasitol. 1975;5:147–57.
38. Wellock IJ, Emmans GC, Kyriazakis I. Modelling the effects of stressors on the performance of poulations of pigs. J Anim Sci. 2004;82:2442–50.

39. Laurenson YCSM, Bishop SC, Kyriazakis I. *In silico* exploration of the mechanisms that underlie parasite-induced anorexia in sheep. Br J Nutr. 2011;106:1023–39.
40. Macfarlane JM, Lewis RM, Emmans GC, Young MJ, Simm G. Predicting carcass composition of terminal sire sheep using X-ray computed tomography. Anim Sci. 2006;82:289–300.
41. Fenton A, Perkins SE. Applying predator-prey theory to modelling immune-mediated, within-host interspecific parasite interactions. Parasitology. 2010;137:1027–38.
42. Bown MD, Poppi DP, Sykes AR. The effect of post-ruminal infusion of protein or energy on the pathophysiology of *Trichostrongylus colubriformis* infection and body composition in lambs. Aust J Agri Res. 1991;42:253–67.
43. Coop RL, Huntley JF, Smith, WD. Effect of dietary protein supplementation on the development of immunity to *Ostertagia circumcincta* in growing lambs. Res Vet Sci. 1995;59:24–9.
44. Coop RL, Kyriazakis I. Nutrition–parasite interaction. Vet Parasitol. 1999;84:187–204.
45. Vanimisetti HB, Andrew SL, Zajac AM, Notter DR. Inheritance of fecal egg count and packed cell volume and their relationship with production traits in sheep infected with *Haemonchus contortus*. J Anim Sci. 2004;82:1602–11.
46. Louie K, Vlassoff A, Mackay A. Nematode parasites of sheep: Extension of a simple model to include host variability. Parasitology. 2005;130:437–46.
47. Elzhov TV, Mullen KM, Spiess AN, Bolker B. R interface to the Levenberg-Marquardt nonlinear least-squares algorithm found in MINPACK, plus support for bounds. 2016.
48. Allen JE, Maizels RM. Diversity and dialogue in immunity to helminths. Nat Rev Immunol. 2011;11:375–88.
49. Buttgereit F, Burmester G-R, Brand MD. Bioenergetics of immune functions: fundamental and therapeutic aspects. Immunol Today. 2000;21:194–9.
50. Mavrot F, Hertzberg H, Torgerson P. Effect of gastro-intestinal nematode infection on sheep performance: a systematic review and meta-analysis. Parasit Vectors. 2015;8:557.
51. Shanebeck KM, Besson AA, Lagrue C, Green SJ. The energetic costs of sub-lethal helminth parasites in mammals: a meta-analysis. Biol Rev. 2022;97:1886–907.
52. Ceï W, Salah N, Alexandre G, Bambou JC, Archimède H. Impact of energy and protein on the gastro-intestinal parasitism of small ruminants: a meta-analysis. Livest Sci. 2018;212:34–44.
53. Méndez-Ortíz FA, Sandoval-Castro CA, Vargas-Magaña JJ, Sarmiento-Franco L, Torres-Acosta JFJ, Ventura-Cordero J. Impact of gastrointestinal parasitism on dry matter intake and live weight gain of lambs: a meta-analysis to estimate the metabolic cost of gastrointestinal nematodes. Vet Parasitol. 2019;265:1–6.
54. Greer AW. Trade-offs and benefits: implications of promoting a strong immunity to gastrointestinal parasites in sheep. Parasite Immunol. 2008;30:123–32.
55. Aguerre S, Jacquiet P, Brodier H, Bournazel JP, Grisez C, Prévot F, et al. Resistance to gastrointestinal nematodes in dairy sheep: Genetic variability and relevance of artificial infection of nucleus rams to select for resistant ewes on farms. Vet Parasitol. 2018;256:16–23.
56. Ramos-Bruno E, Torres-Acosta JFJ, Sarmiento-Franco LA, Sandoval-Castro CA. Metabolizable energy balance in hair sheep lambs artificially infected with *Haemonchus contortus*. Vet Parasitol. 2021;300:109620.
57. Liu SM, Smith TL, Karlsson LJE, Palmer DG, Besier RB. The costs for protein and energy requirements by nematode infection and resistance in Merino sheep. Livest Prod Sci. 2005;97:131–9.
58. Hall SR, Simonis JL, Nisbet RM, Tessier AJ, Cáceres CE. Resource ecology of virulence in a planktonic host-parasite system: an explanation using dynamic energy budgets. Am Nat. 2009;174:149–62.
59. Vagenas D, Bishop SC, Kyriazakis I. A model to account for the consequences of host nutrition on the outcome of gastrointestinal parasitism in sheep: logic and concepts. Parasitology. 2007;134:1263–77.
60. Doeschl-Wilson AB, Vagenas D, Kyriazakis I, Bishop SC. Exploring the assumptions underlying genetic variation in host nematode resistance. Genet Sel Evol. 2008;40:241–64.
61. Saccareau M, Moreno CR, Kyriazakis I, Faivre R, Bishop SC. Modelling gastrointestinal parasitism infection in a sheep flock over two reproductive seasons: *in silico* exploration and sensitivity analysis. Parasitology. 2016;143:1509–31.
62. Sandberg FB, Emmans GC, Kyriazakis I. Partitioning of limiting protein and energy in the growing pig: description of the problem, possible rules and their qualitative evaluation. Br J Nutr. 2005;93:205–12.
63. Doeschl-Wilson AB, Brindle W, Emmans G, Kyriazakis I. Unravelling the relationship between animal growth and immune response during micro-parasitic infections. PLoS ONE. 2009;4:e7508.
64. Colditz IG. Six costs of immunity to gastrointestinal nematode infections. Parasite Immunol. 2007;30:63–70.
65. Verschave SH, Charlier J, Rose H, Claerebout E, Morgan ER. Cattle and nematodes under global change: transmission models as an ally. Trends Parasitol. 2016;32:724–38.
66. Prada Jiménez de Cisneros J, Stear MJ, Mair C, Singleton D, Stefan T, Stear A, et al. An explicit immunogenetic model of gastrointestinal nematode infection in sheep. J R Soc Interface. 2014;11:20140416.
67. Bartlett LJ, Wilfert L, Boots M. A genotypic trade-off between constitutive resistance to viral infection and host growth rate. Evolution. 2018;72:2749–57.
68. van der Most PJ, de Jong B, Parmentier HK, Verhulst S. Trade-off between growth and immune function: a meta-analysis of selection experiments. Funct Ecol. 2011;25:74–80.
69. Tate AT, Graham AL. Dynamic patterns of parasitism and immunity across host development influence optimal strategies of resource allocation. Am Nat. 2015;186:495–512.
70. Martin AR, Tate AT. Pleiotropy alleviates the fitness costs associated with resource allocation trade-offs in immune signaling networks. Proc R Soc B. 2024;291:20240446.
71. Hamilton R, Siva-Jothy M, Boots M. Two arms are better than one: parasite variation leads to combined inducible and constitutive innate immune responses. Proc R Soc B. 2008;275:937–45.
72. Sivakumaran S, Agakov F, Theodoratou E, Prendergast JG, Zgaga L, Manolio T, et al. Abundant pleiotropy in human complex diseases and traits. Am J Hum Genet. 2011;89:607–18.
73. Greer AW, Hamie JC. Relative maturity and the development of immunity to gastrointestinal nematodes in sheep: an overlooked paradigm? Parasite Immunol. 2016;38(5):263–72.
74. McKean KA, Yourth CP, Lazzaro BP, Clark AG. The evolutionary costs of immunological maintenance and deployment. BMC Evol Biol. 2008;8:76.
75. McKean KA, Lazzaro BP. The costs of immunity and the evolution of immunological defense mechanisms. In: Flatt T, Heyland A, editors. Mechanisms of life history evolution. Oxford: Oxford University Press; 2011. p. 299–310.
76. Garland TJ. Selection experiments: an under-utilized tool in biomechanics and organismal biology. In: Bels VL, Gasc JP, Casinos A, editors. Vertebrate Biomechanics and Evolution. Oxford: BIOS Scientific Publishers Ltd; 2003. p. 23–56.
77. Leitão AB, Arunkumar R, Day JP, Geldman EM, Morin-Poulard I, Crozatier M, et al. Constitutive activation of cellular immunity underlies the evolution of resistance to infection in *Drosophila*. eLife. 2020;9:e59095.
78. Lazzaro BP. Adenosine signaling and the energetic costs of induced immunity. PLoS Biol. 2015;13:e1002136.
79. Weibel ER, Taylor CR, Hoppeler H. The concept of symmorphosis: a testable hypothesis of structure-function relationship. Proc Natl Acad Sci USA. 1991;88:10357–61.
80. Cohen AA, Martin LB, Wingfield JC, McWilliams SR, Dunne JA. Physiological regulatory networks: ecological roles and evolutionary constraints. Trends Ecol Evol. 2012;27:428–35.
81. Tate AT, Schulz NK. The within-host ecology of insects and their parasites: integrating experiments and mathematical models. Curr Opin Insect Sci. 2022;49:37–41.

Publisher's Note